Journal of Power Sources 189 (2009) 494–498

Contents lists available at ScienceDirect

Journal of Power Sources

journal homepage: www.elsevier.com/locate/jpowsour

Short communication

Effect of protecting metal oxide (Co_3O_4) layer on electrochemical properties of spinel $Li_{1.1}Mn_{1.9}O_4$ as a cathode material for lithium battery applications

Ki-Soo Lee [a], Seung-Taek Myung [b,**], Hyunjoo Bang [a], Khaili Amine [c], Dong-Won Kim [a], Yang-Kook Sun [a,*]

[a] Department of Chemical Engineering, Center for Information and Communication Materials, Hanyang University, Seoul 133-791, South Korea
[b] Department of Chemical Engineering, Iwate University, 4-3-5 Ueda, Morioka, Iwate 020-8551, Japan
[c] Electrochemical Technology Program, Chemical Engineering Division, Argonne National Laboratory, Argonne, IL 60493, USA

ARTICLE INFO

Article history:
Received 25 July 2008
Received in revised form
18 November 2008
Accepted 18 November 2008
Available online 25 November 2008

Keywords:
Co_3O_4
Spinel
$Li_{1.1}Mn_{1.9}O_4$
Cathode
Lithium
Battery

ABSTRACT

Metal oxide (Co_3O_4) was coated on spinel $Li_{1.1}Mn_{1.9}O_4$ using glutamic acid. Powder X-ray diffraction pattern of Co_3O_4-coated spinel $Li_{1.1}Mn_{1.9}O_4$ showed that the Co_3O_4 coating medium was not incorporated in the spinel bulk structure. Morphology of the Co_3O_4-coated spinel $Li_{1.1}Mn_{1.9}O_4$ was observed by scanning electron microscopy and transmission electron microscopy. The cycling performance of the Co_3O_4-coated spinel $Li_{1.1}Mn_{1.9}O_4$ was obviously improved, compared to the pristine $Li_{1.1}Mn_{1.9}O_4$ at elevated temperature (55 °C). Improvement of rate capability was also achieved at high C-rates.

1. Introduction

Due to great increase in fossil fuel price a great deal of attention, recently, has been paid to Li-ion batteries as assistant or power sources for vehicles. To meet the requirements for hybrid electric vehicles (HEVs) such as reliable power, capacity, safety, and so on, manganese-based spinel $Li_{1+x}Mn_{2-x}O_4$ and its derivatives have been received extensive attentions due to economical advantage and excellent power performance [1]. However, manganese spinel materials have an inherent drawback: the disproportionated Mn dissolution ($2Mn^{3+} \rightarrow Mn^{2+} + Mn^{4+}$) [2].

To overcome capacity fading upon cycling, a lot of trials were made; the manganese site replacement by other elements, $LiMMn_{2-x}O_4$ (M = Li, Al, Co, Ni, Fe, Cr, Zn, etc.) to enhance structural stability [3–10]. The capacity fading was obviously suppressed as the amount of dopant increased causing decrease of delivered capacity comparing to undoped $LiMn_2O_4$. Komaba et al. [9] suggested that $Li_{1.1}Mn_{1.9}O_4$ significantly suppressed the Mn dissolution due to stabilizing of the host structure by substituting Li for Mn in $LiMn_2O_4$. Many research groups have also studied to improve the poor capacity retention of the spinel material with anion substitution into spinel structure [11,12].

Recently, surface modifications with various metal oxides and metal fluorides on cathode materials have been reported [13–24]. Those treatments presented significantly improved results such as rate capabilities, cyclability, etc. in spinel and several compound. Myung et al. [15,16] suggested that an Al_2O_3 coating layer on $Li[Li_{0.05}Ni_{0.4}Co_{0.15}Mn_{0.4}]O_2$ particles gradually transformed to AlF_3 through an intermediate complex of an Al–O–F compound, as confirmed by time of flight-secondary ion mass spectroscopy. Sun et al. [17,18] reported that an AlF_3 coating layer would act as an interfacial stabilizer, as found by an electrochemical impedance spectroscopy. In this study, we prepared surface-modified spinel $Li_{1+x}Mn_{2-x}O_4$ followed by Co_3O_4 coating. Electrochemical performance of the as-prepared and the metal oxide-coated spinel materials were evaluated.

2. Experimental

Mn_3O_4 powder was synthesized by co-precipitation method [25]. The prepared precursor Mn_3O_4 containing an excess amount of $LiOH{\cdot}H_2O$ (molar ratio of Li:Mn = 0.55), were preheated to 500 °C for 5 h in oxygen, and subsequently heat treated for 15 h at 850 °C in a furnace under oxygen purging. Co-oxide coating (0.3 wt%) on

* Corresponding author. Tel.: +82 2 2220 0524; fax: +82 2 2282 7329.
** Corresponding author. Tel.: +81 19 621 6345; fax: +81 19 621 6345.
E-mail addresses: smyung@iwate-u.ac.jp (S.-T. Myung), yksun@hanyang.ac.kr (Y.-K. Sun).

0378-7753/$ – see front matter © 2008 Published by Elsevier B.V.
doi:10.1016/j.jpowsour.2008.11.062

$Li_{1.1}Mn_{1.9}O_4$ material was carried out in cobalt hydroxide containing solution in the presence of glutamic acid. To maintain proper pH during the coating process, ammonia solution was fed into the solution until pH 7. After continuous mixing for 2 h, the metal oxide-coated $Li_{1.1}Mn_{1.9}O_4$ powders were filtered and washed with distilled water several times. The obtained powders, thus, were heated at 500 °C for 5 h in an air.

Powder X-ray diffraction (Rigaku, Rint-2000) using Cu Kα radiation was used to identify crystalline phase of the prepared powders at each stage. The collected intensity data of XRD were analyzed by the Rietveld refinement program *Fullprof* 2002 [26]. $Co(OH)_2$ as the starting coating material was examined by a thermal gravimetric analysis (TG, DTG-60, SHIMADZU, Japan) with 1 °C min^{-1} of heating. The morphology of prepared powders was also observed using scanning electron microscopy (SEM, JSM-6340F, JEOL). A transmission electron microscopy (TEM, JEM2010, JEOL) was employed to characterize the prepared powders. Chemical compositions of the final products were analyzed with an atomic absorption spectroscopy (AAS, Vario 6, Analyticjena).

The coin cells comprised of the prepared powder as a cathode, lithium foil as an anode, and an electrolyte having 1 M $LiPF_6$ in ethylene carbonate and diethyl carbonate (1:1 in volume, Cheil Industries Inc. Korea). Micro-porous polypropylene separator was used in those cells. The cell preparation was carried out in an Ar-filled dry box. Charge–discharge tests were performed with 2032 coin type cell by applying a constant current density of 100 mA g^{-1} (1 C-rate) in voltage range of 3.0–4.3 V at 55 °C.

3. Results and discussion

To determine the Co-oxide coating on the crystal structure of the spinel materials, the X-ray powder diffraction were carried out for uncoated spinel (pristine) and the coated spinel materials. Fig. 1 shows the XRD patterns of the pristine and Co-oxide-coated spinel materials. The prisine spinel material has a typical spinel phase with *Fd*3*m* space group in Fig. 1a. There is no significant change in the XRD pattern for the coated spinel material in Fig. 1b, compared with the pristine. Calculated lattice parameter by Rietveld refinement was $a = 8.215(5)$ Å for both materials, of which the value is close to that of reported [9]. No change in the lattice parameter for both samples suggested that Co was not incorporated into the bulk structure of the coated spinel. To figure out the possible chemical composition of the coating layer, thermal gravimetric examination for the starting $Co(OH)_2$ was carried out in Fig. 1d. A drastic weight loss is seen from 200 °C due to evaporation of water molecules from the $Co(OH)_2$. Then, a steady decrease in the weight is seen to 500 °C, which is attributed to a gradual phase transformation. Hence, we decided that the temperature is the best point for the heat-treatment temperature after coating procedure. As confirmed by XRD in Fig. 1c, one can clearly observe that calcination of the $Co(OH)_2$ at 500 °C for 5 h exhibited a well-crystallized cubic spinel Co_3O_4. Therefore, it is believed that the spinel $Li_{1.1}Mn_{1.9}O_4$ shown in Fig. 1b is coated by Co_3O_4. Absent of Co_3O_4-related peak in Fig. 1b is due to the little amount of Co_3O_4 (~0.3 wt%) in the Co_3O_4-coated final product. Again, no change in the lattice parameter was observed, implying the Co_3O_4 coating medium was not incorporated into the spinel structure but is just presented on the surface of $Li_{1.1}Mn_{1.9}O_4$, since Co^{3+} introduction into the spinel structure leads to change of the lattice parameter. Furthermore, calcination temperature, 500 °C, to get the crystalline Co_3O_4 is too low temperature for Co to be diffused into the spinel lattice, forming Co-doped $Li_{1.1}Mn_{1.9}O_4$.

Morphologies of the pristine and Co_3O_4-coated spinel material observed by SEM are shown in Fig. 2. A very small amount of Co_3O_4 would be hard to be detected by XRD in Fig. 1b. Existence

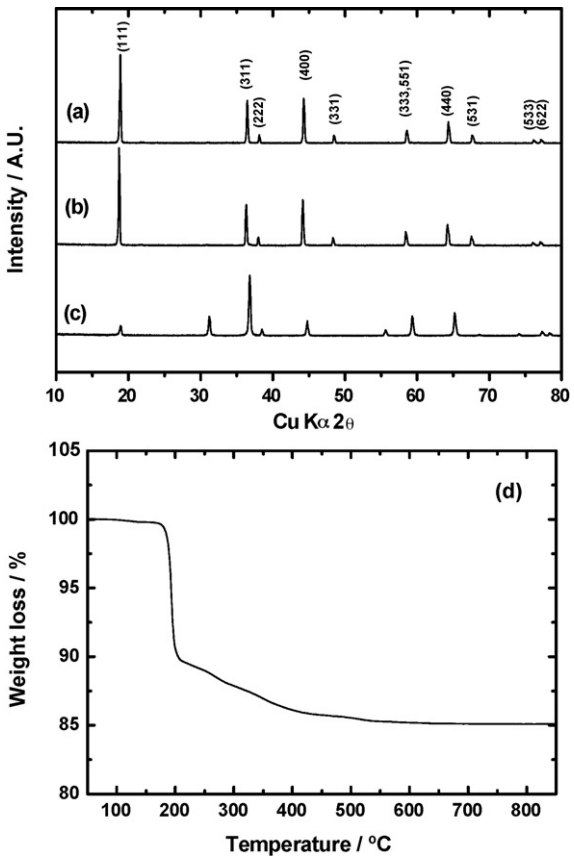

Fig. 1. XRD patterns of as-prepared (a) $Li_{1.1}Mn_{1.9}O_4$, (b) Co_3O_4-coated $Li_{1.1}Mn_{1.9}O_4$, (c) Co_3O_4 produced from calcination of $Co(OH)_2$, and (d) thermalgravimetric curve of $Co(OH)_2$ as the coating medium.

of the Co_3O_4 particles on the spinel particle was clearly visible and they are well dispersed on the surface of spinel particles (Fig. 2b), compared to the pristine spinel particles (Fig. 2a). At lower magnification in Fig. 2c, one can observe that the as-prepared $Li_{1.1}Mn_{1.9}O_4$ has a spherical morphology and the particle is approximated to 10 μm in the secondary morphology. As observed in Fig. 2d and e, the material contains Mn element and Co ingredient are also uniformly dispersed on the surfaces of particles.

Fig. 3 illustrates TEM bright-field images of the pristine and Co_3O_4-coated $Li_{1.1}Mn_{1.9}O_4$. The pristine material shows a very smooth edge line, and there is no other layer on the surface in Fig. 3a. As expected, it is clearly observed that Co_3O_4 layer having its thickness of 20 nm was coated on the surface of $Li_{1.1}Mn_{1.9}O_4$. The uniform contrast of the Co_3O_4 layer implies that the Co_3O_4 coating layer is thin and uniform.

Provided that the coating medium is incorporated into the spinel $Li_{1.1}Mn_{1.9}O_4$ structure, the Co element as a trivalent would occupy 16*d* Mn sites to replace Mn^{3+} (0.65 Å [27], high spin) and/or Mn^{4+} (0.54 Å [27]). However, it usually happens during high temperature calcinations (700–900 °C) for a long time. If the Co element was substituted for Mn, it is natural to change the lattice parameter due to the difference in the ionic radii of Co^{3+} (0.535 Å [27], low spin) relative to Mn^{3+} (0.65 Å [27], low spin). Furthermore, the main driving force, heating temperature, was only 500 °C which is too low to incorporate Co^{3+} element into the spinel structure and the dwelling time as well (5 h). Again, the lattice parameter was not changed, compared with pristine $Li_{1.1}Mn_{1.9}O_4$. Those things are very strong clues that the formed Co_3O_4 coating medium was not introduced into the structure, but is just remained on the surface of spinel $Li_{1.1}Mn_{1.9}O_4$.

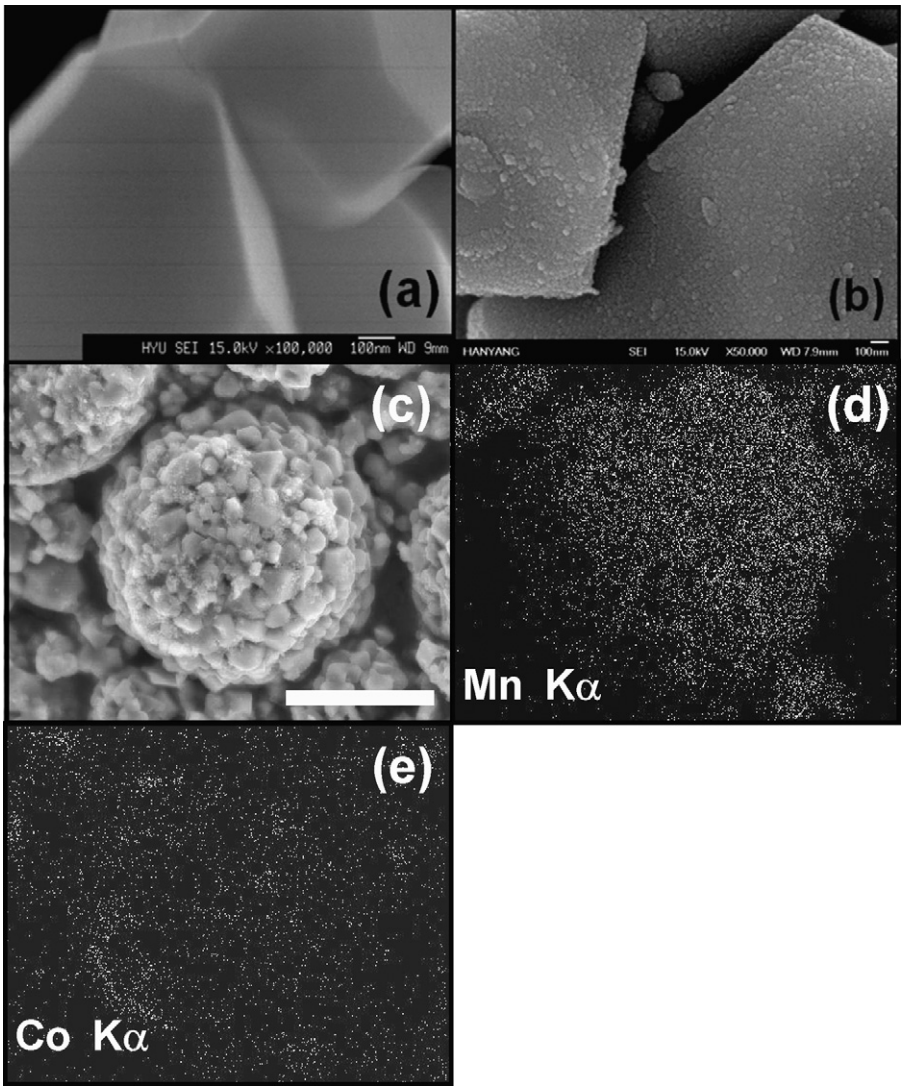

Fig. 2. SEM images of as-prepared (a) $Li_{1.1}Mn_{1.9}O_4$, (b) Co_3O_4-coated $Li_{1.1}Mn_{1.9}O_4$ with high magnification (×100,000), (c) Co_3O_4-coated $Li_{1.1}Mn_{1.9}O_4$ with low magnification (×4000) (scale bar: 5 μm) and corresponding energy dispersive spectroscopic mapping of (d) Mn and (e) Co elements.

Fig. 4 shows the initial charge and discharge profiles for Li/pristine $Li_{1.1}Mn_{1.9}O_4$ and Li/Co_3O_4-coated $Li_{1+x}Mn_{2-x}O_4$ cells at constant current of 50 mA cm^{-2} at 55 °C over the voltage range of 3.0–4.3 V. The pristine $Li_{1.1}Mn_{1.9}O_4$ shows a specific discharge capacity of about 107.4 mAh g^{-1}. Comparing to the pristine $Li_{1.1}Mn_{1.9}O_4$, the Co_3O_4-coated $Li_{1.1}Mn_{1.9}O_4$ cell exhibited a little lower capacity of 105.1 mAh g^{-1}. Provided that the Mn element is replaced by Co from Co_3O_4, the resulting voltage profile would be

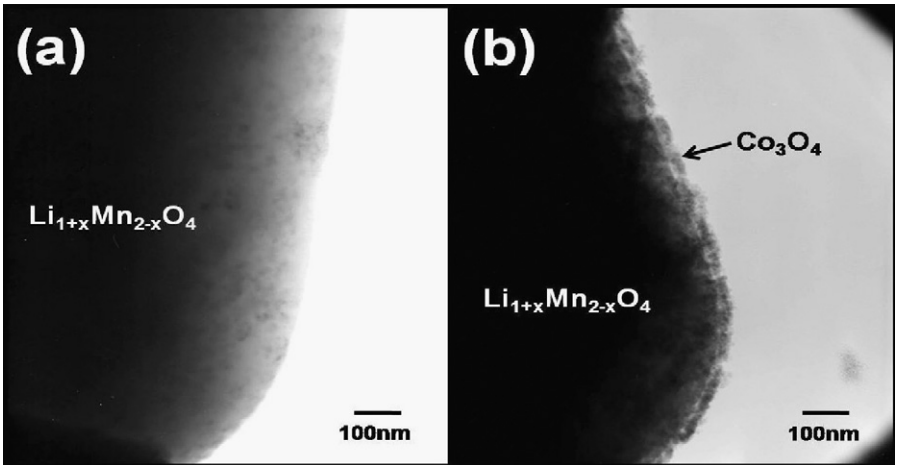

Fig. 3. TEM images of as-prepared (a) $Li_{1.1}Mn_{1.9}O_4$ and (b) Co_3O_4-coated $Li_{1.1}Mn_{1.9}O_4$.

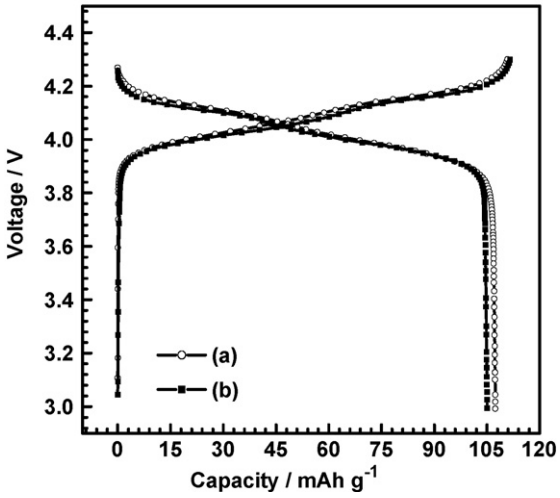

Fig. 4. Initial charge and discharge profiles of (a) $Li_{1.1}Mn_{1.9}O_4$ and (b) Co_3O_4-coated $Li_{1.1}Mn_{1.9}O_4$ at a current level of 0.5 C (50 mA g^{-1}) at 55 °C.

changed due to different interaction between lithium positive and positive ions in the oxide lattice by the Co incorporation, as Myung et al. previously clarified in $LiAl_xMn_{2-x}O_4$ spinel system [3]. In fact, the voltage profile is almost similar for both materials in Fig. 4, which indicates that the Co_3O_4 was not incorporated into the spinel structure.

The cycling performances of pristine $Li_{1.1}Mn_{1.9}O_4$ and Co_3O_4-coated $Li_{1.1}Mn_{1.9}O_4$ cells at 100 mA g^{-1} (1 C-rate) in the voltage range of 3.0–4.3 V at 55 °C are seen in Fig. 5. As expected, the pristine $Li_{1.1}Mn_{1.9}O_4$ presented a gradual capacity fading upon cycling. This tendency would result from the reaction with HF that is generated by decomposition of electrolytic salt, $LiPF_6$. In fact, electrolyte always contains a small amount of water content such as ≤50 ppm. As cycle goes by, electrolytic salts are decomposed, as we have suggested [15,16,28]. The formed HF attacks active material so that the following reaction occurs: $MnO + 2HF \rightarrow MnF_2 + H_2O$ [15,16,28]. This means that after HF attack the most outer surface is transformed to metal fluoride layer. Meanwhile, this reaction generates water molecules. The formed water molecular also reacts with electrolyte salt again, $LiPF_6$, and it, ceaselessly, lead to decomposition of electrolytic salt, propagating more amount of HF.

Since the propagation of HF is facilitated at elevated temperature, damage of the spinel active material accompanying by the disproportionated dissolution of Mn at the temperature can affect

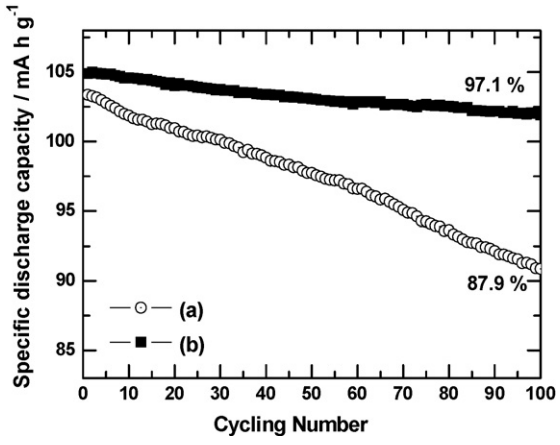

Fig. 5. Cycling performances of (a) $Li_{1.1}Mn_{1.9}O_4$ and (b) Co_3O_4-coated $Li_{1.1}Mn_{1.9}O_4$ at a current level of 1 C (100 mA g^{-1}) in the voltage range of 3.0–4.3 V at 55 °C.

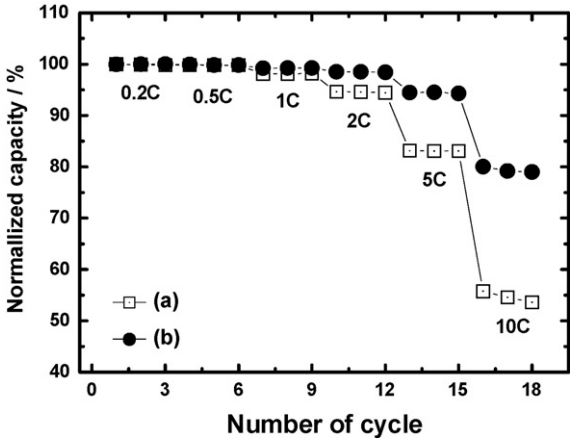

Fig. 6. Corresponding specific discharge capacities of (a) $Li_{1.1}Mn_{1.9}O_4$ and (b) Co_3O_4-coated $Li_{1.1}Mn_{1.9}O_4$ cell at various current densities between 3.0 and 4.3 V.

the decrease in the discharge capacity from earlier stage, as an obvious occurrence of capacity fading during cycling is seen in Fig. 5a. The capacity retention was relatively poor, but about 87.9% of its initial capacity was kept during cycling. For the Co_3O_4-coated $Li_{1.1}Mn_{1.9}O_4$, surprisingly, the retained capacity after cycling was of about 97.1% of its initial discharge capacity in Fig. 5b, although a slight capacity loss appeared during cycling. Once the active material is exposed to the acidic species such as HF that is generated by the decomposition of electrolytic salt, $LiPF_6$, the active material can be relatively readily deteriorated by the HF attack during cycling, resulting in serious disproportionated reaction of Mn element. For example, as is well known, Mn^{4+} would reside with active material as electro-inactive Li_2MnO_3 that makes discontinuous network of electron transfer. Mn^{2+} would be deposited on the surface of negative electrode and it is spontaneously reduced to metallic compound. This combination, in turn, deteriorates cell performances with increased cell impedance. From the cycling results shown in Fig. 5b, it seems that those reactions would be suppressed by the Co_3O_4 coating on the surface of spinel compound. The Co_3O_4 coating layer would react with the generated HF, it is expected that the reaction finally gives rise to the formation of Co-F layer on the most outer surface, based on our previous ToF-SIMS results [15,16]. This would imply that though the same amount of HF is generated into the electrolyte in the cell during the cycling, the presence of the Co_3O_4 coating layer join to trap the F^- from HF, leading to fewer amount of HF propagation relative to that of pristine $Li_{1.1}Mn_{1.9}O_4$, which, in turn, makes it possible to reduce resistance on interface. Therefore, the higher discharge capacity could be successfully maintained by employing Co_3O_4 coating onto $Li_{1.1}Mn_{1.9}O_4$.

Comparison of rate capability for the pristine and Co_3O_4-coated $Li_{1.1}Mn_{1.9}O_4$ cells is shown in Fig. 6. The cells were charged with a current density of 20 mA g^{-1} (0.2 C-rate) before each discharge test. The Co_3O_4-coated $Li_{1.1}Mn_{1.9}O_4$ electrode exhibited a higher discharge capacity than the pristine electrode at higher C-rate. At 5 C-rates, the delivered capacities of pristine and Co_3O_4-coated electrodes were 89.2 mAh g^{-1} and 100.5 mAh g^{-1}, respectively. The capacity of pristine and Co_3O_4-coated electrode at 10 C-rate were each 55% and 79% of the capacity at 0.2 C-rate.

4. Conclusions

$Li_{1.1}Mn_{1.9}O_4$ was synthesized using metal oxide precursor by co-precipitation method. XRD revealed that the prepared $Li_{1.1}Mn_{1.9}O_4$ and Co_3O_4-coated $Li_{1.1}Mn_{1.9}O_4$ had a phase pure single phase spinel structure with *Fd*3*m* space group. The Co_3O_4 coating did not result in change in the host structure of $Li_{1.1}Mn_{1.9}O_4$. Co_3O_4 particles

are uniformly dispersed on the surface of spinel $Li_{1.1}Mn_{1.9}O_4$ particles. Based on the TEM image, the estimated coating layer was about 20 nm in thickness. The Co_3O_4-coated $Li_{1+x}Mn_{2-x}O_4$ electrode exhibited an excellent cycle performance in the voltage range of 3.0–4.3 V at elevated temperature (55 °C). The capacity retention of Co_3O_4-coated $Li_{1.1}Mn_{1.9}O_4$ electrode over 100 cycles was 97.1%, while pristine showed 87.9% capacity retention of the initial discharge capacity. The rate capability of the Co_3O_4-coated $Li_{1.1}Mn_{1.9}O_4$ electrode was superior to the uncoated $Li_{1.1}Mn_{1.9}O_4$ at higher C-rate as well.

Acknowledgement

This research was supported by Korea Institute of Energy and Resources Technology Evaluation and Planning.

References

[1] T. Ohzuku, M. Kitagawa, T. Hirai, J. Electrochem. Soc. 137 (1990) 769.
[2] D.H. Jang, Y.J. Shin, S.M. Oh, J. Electrochem. Soc. 143 (1996) 2204.
[3] S.-T. Myung, S. Komaba, N. Kumagai, J. Electrochem. Soc. 148 (2001) A482.
[4] B. Banov, Y. Todorov, A. Trifonova, A. Momchilov, V. Manev, J. Power Sources 68 (1997) 578.
[5] Y.-K. Sun, G.-S. Park, Y.-S. Lee, M. Yoshio, K.-S. Nahm, J. Electrochem. Soc. 148 (2001) A994.
[6] K. Amine, H. Tukamoto, H. Yasuda, Y. Fujita, J. Electrochem. Soc. 143 (1996) 1607.
[7] C. Sigala, A. Vebaere, J.L. Mansot, D. Guyomard, Y. Piffard, T. Tournoux, J. Solid State Chem. 132 (1997) 372.
[8] K. Amine, H. Tukamoto, H. Yasuda, Y. Fujita, J. Power Sources 68 (1997) 604.
[9] S. Komaba, N. Kumagai, T. Sasaki, Y. Miki, Electrochemical 69 (2001) 784.
[10] L. Hernan, J. Morales, L. Sanchez, J. Santos, Solid State Ionics 118 (1999) 179.
[11] Y.-K. Sun, Y.-S. Jeon, H.-J. Lee, Electrochem. Solid-State Lett. 3 (2000) 7.
[12] S.-H. Park, K.-S. Park, Y.-K. Sun, K.-S. Nahm, J. Electrochem. Soc. 147 (2000) 2116.
[13] Y.-K. Sun, Y.-S. Lee, M. Yoshio, K. Amine, Electrochem. Solid-State Lett. 5 (2002) A99.
[14] Z. Chen, J.R. Dahn, Electrochim. Acta 49 (2004) 1079.
[15] S.-T. Myung, K. Izumi, S. Komaba, Y.-K. Sun, H. Yashiro, N. Kumagai, Chem. Mater. 17 (2005) 3695.
[16] S.-T. Myung, K. Izumi, S. Komaba, H. Yashiro, H.J. Bang, Y.-K. Sun, N. Kumagai, J. Phys. Chem. C 111 (2007) 4061.
[17] Y.-K. Sun, J.-M. Han, S.-T. Myung, S.-W. Lee, K. Amine, Electrochem. Commun. 8 (2006) 821.
[18] B.-C. Park, H.-B. Kim, S.-T. Myung, K. Amine, I. Belharouak, S.-M. Lee, Y.-K. Sun, J. Power Sources 178 (2008) 826.
[19] S.-S. Kim, Y. Kadoma, H. Ikuta, Y. Uchimoto, M. Wakihara, Electrochem. Solid State Lett. 4 (2001) A109.
[20] I.R.M. Kottegoda, Y. Kadoma, H. Ikuta, Y. Uchimoto, M. Wakihara, Electrochem. Solid State Lett. 5 (2002) A275.
[21] A. Eftekhari, J. Electrochem. Soc. 151 (2004) A1456.
[22] J. Cho, Y.J. Kim, B. Park, J. Electrochem. Soc. 148 (2001) A1110.
[23] J. Cho, Y.J. Kim, T.J. Kim, B. Park, Angew. Chem. Int. Ed. Engl. 40 (2001) 3367.
[24] Z. Chen, J.R. Dahn, Electrochem. Solid-State Lett. 5 (2002) A213.
[25] K.-S. Lee, S.-T. Myung, H.-J. Bang, S.-J. Chung, Y.-K. Sun, Electrochim. Acta 52 (2007) 5201.
[26] T. Roisnel, J. Rodriguez-Carjaval, Fullprof Manual, Institut Laue- Langevin, Grenoble, France, 2002.
[27] R.D. Shannon, Acta Crystallogr. Sect. A: Cryst. Phys. Diffr. Theor. Gen. Crystallogr. 32 (1976) 756.
[28] S.-T. Myung, K. Hosoya, S. Komaba, H. Yashiro, Y.-K. Sun, N. Kumagai, Electrochim. Acta 51 (2006) 5912.